Role of negative-parity resonances in the electromagnetic weak $\Sigma^+ \to p\gamma$ decay

I. Picek
"Rudjer Bošković" Institute, Zagreb, Croatia, Yugoslavia
(Received 27 December 1979)

Contributions from $1/2^-$ resonance poles to the parity-violating amplitude for $\Sigma^+ \to p\gamma$ have been estimated. Two-quark weak transitions have been described in the framework of the Weinberg-Salam model including quantum-chromodynamics corrections. Weak matrix elements and photon emissions have been calculated using the MIT bag model. It has been shown that $1/2^-$ resonance poles give sizable contributions, which might provide an explanation of the experimental results.

I. INTRODUCTION

Recent papers[1,2] on electromagnetic weak baryon decays can serve as a motivation for reconsidering the only radiative weak decay for which the asymmetry parameter has been measured.[3] This decay $\Sigma^+ \to p\gamma$ was used as an input[1] to rule out recent models[4] based on single-quark transitions $s \to d\gamma$ (Fig. 1) and to suggest models based on two-quark transitions (Fig. 2). Our approach belongs to the type of models shown in Fig. 2; it is a model based on baryon poles, as represented schematically in Fig. 3. Baryon poles of interest are those of negative-parity baryon resonances. The weak vertex in Fig. 3 is determined by the Weinberg-Salam model including quantum-chromodynamics (QCD) renormalization effects and SU(4)-flavor-symmetry breaking.[5] It has been concluded[5] that such a description combined with the MIT bag model[6,7] leads to a successful description of nonleptonic decays.[8] In this way, one obtains the effective weak couplings which, together with the effective electromagnetic couplings calculated in the MIT bag model, enter the parity-violating (PV) amplitude of the general electromagnetic-weak interaction[9]

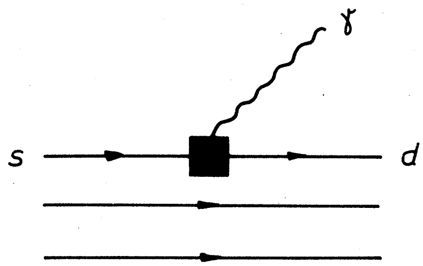

FIG. 1. Radiative weak decays based on the single-quark transition $s \to d\gamma$. The black box represents short-distance-type models (Ref. 4).

$$H^{\mathrm{eff}}_{\mathrm{WEM}} = \tfrac{1}{2} e\, \overline{\Psi}_p(x)\, (C + D\gamma_5)\sigma_{\mu\nu}\Psi_{\Sigma^+}(x) F_{\mu\nu}(x) + \mathrm{H.c.} \tag{1a}$$

The expressions for the decay rate Γ and for the asymmetry parameter α are of the form

$$\Gamma = (e^2/\pi)\, k^3 (C^2 + D^2) \tag{1b}$$

and

$$\alpha = 2\frac{CD}{C^2 + D^2}\,. \tag{1c}$$

The energy of the outgoing photon is $k = (m_{\Sigma^+}{}^2 - m_p{}^2)/2m_{\Sigma^+}$. In this paper we use the phase convention of Ref. 9 and choose C and D to be real.

II. $\frac{1}{2}^-$ BARYON POLES CONTRIBUTING TO THE PV AMPLITUDE

According to the MIT bag model,[6,7] negative-parity baryon resonances contribute only to PV amplitudes. It has been shown[10] that these resonances may play an important role in explaining the $NN\rho$ PV amplitude. On the other hand, these resonances are the missing part in previous pole calculations[11] and in a recent one.[2] Therefore, our PV amplitudes can be simply added, for example, to those of Ref. 2.

Figure 4 shows pole-model diagrams for $\frac{1}{2}^-$ baryon resonances relevant for the $\Sigma^+ \to p\gamma$ decay. The symbols N^* (Σ^*) denote nonstrange (strange)

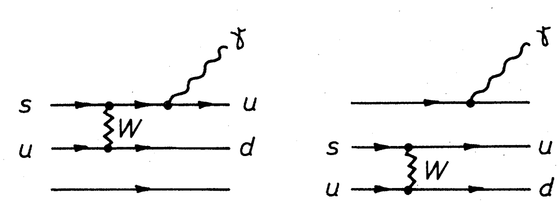

FIG. 2. Examples of two-quark-transition radiative weak decays.

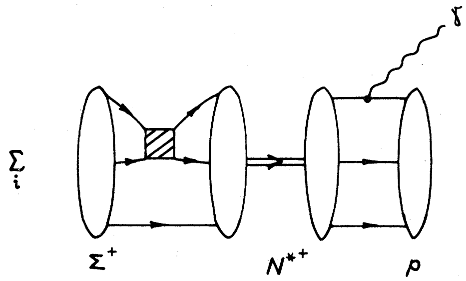

FIG. 3. Scheme of our calculational approach. The shaded box represents the weak Hamiltonian [Eq. (3)]. The sum extends over all possible quark lines. The double line is a $\frac{1}{2}^-$ resonance propagator.

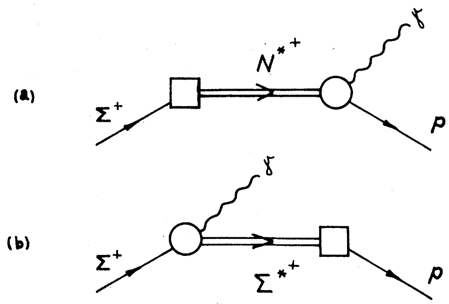

FIG. 4. Pole diagrams of negative-parity baryons. The box represents the weak Hamiltonian [Eq. (5)] and the circle the electromagnetic Hamiltonian [Eq. (7)].

resonances. Particle data[12] provide three nonstrange resonances, S'_{11} (1535), S''_{11} (1700), and S'_{31} (1650), and one strange resonance, S''_{11} (1750). On the other hand, the model we are using[13] predicts three nonstrange states, $N^* = \{N_a(1327), N_b(1275), \Delta(1362)\}$, and three strange states, $\Sigma^* = \{\Sigma_1(1445), \Sigma_a(1517), \Sigma_b(1473)\}$. The respective contributions from these states to the PV amplitude in Eqs. (1) are given by

$$eD(N^*) = -\frac{E(N^*)\mu_T(N^*)}{m_{N^*} - m_{\Sigma^+}} \tag{2a}$$

and

$$eD(\Sigma^*) = \frac{E(\Sigma^*)\mu_T(\Sigma^*)}{m_{\Sigma^*} - m_p} . \tag{2b}$$

The couplings E and μ_T, which characterize weak and electromagnetic vertices, are calculated in Secs. III and IV, respectively.

III. WEAK VERTICES

A. The effective weak Hamiltonian

The weak $\Delta S = 1$ transition $\Sigma \to N^*$ ($N^* \to p$) can be calculated using the effective weak Hamiltonian based on the Weinberg-Salam model and renormalized by QCD effects, including SU (4)-symmetry breaking (the so-called penguin terms)[5]:

$$(H_W^{\Delta S=1})_{\text{eff}} = \sqrt{2}\, G_F \sin\theta_C \cos\theta_C \sum_{i=1}^{6} C_i O_i . \tag{3}$$

The operators O_i appearing in expression (3) are normal-ordered sums of several four-quark combinations. We represent them in a comprehensible form in Table I. The symbols L and R have the following meaning:

$$(\bar{q}_L^1 q_L^2)(\bar{q}_L^3 q_L^4) = -\tfrac{1}{4}[(\bar{q}^1 q^2)(\bar{q}^3 q^4)]_{VA+AV} , \tag{4a}$$

$$(\bar{q}_L^1 q_L^2)(\bar{q}_R^3 q_R^4) = \tfrac{1}{4}[(\bar{q}^1 q^2)(\bar{q}^3 q^4)]_{VA-AV} . \tag{4b}$$

We summarize the values of the coefficients C_i in Eq. (A1).

B. Calculation of matrix elements

In Fig. 3 we illustrate the determination of the effective weak vertices $E(N^*)$ appearing in the pole diagram in Fig. 4(a). Equivalently, we determine $E(\Sigma^*)$ appearing in the pole diagram in Fig. 4(b) by calculating the matrix elements of Eq. (3) between the proton state and the strange $\frac{1}{2}^-$ resonance state. In this way, we obtain the effective Hamiltonian density of the $\Delta S = 1$ $\frac{1}{2}^- \to \frac{1}{2}^+$ weak transition:

$$[H_W^{\Delta S=1}(x)]^{\text{PV}} = \sum_{N^*} [E(N^*)\bar{\Psi}_{N^*}(x)\Psi_\Sigma(x) + \text{H.c.}] + \sum_{\Sigma^*} [E(\Sigma^*)\bar{\Psi}_p(x)\Psi_{\Sigma^*}(x) + \text{H.c.}] . \tag{5}$$

We calculate the matrix elements by using the MIT-bag-model wave function. Our description of $\frac{1}{2}^-$ resonances, which we summarize in the Appendix [see formulas (A2) and (A3)], is entirely based on Ref. 13. The explicit structure of these states allows the contributions only from the first two quark combinations in Table I [i.e., $(\bar{d}s)$ $(\bar{u}u)$ and $(\bar{d}u)$ $(\bar{u}s)$, where each q contains an s- and a p-wave part]. According to formula (4), the matrix elements of these combinations (denoted below by M and N, respectively) build up the matrix elements of the operators from Table I as follows:

$$\langle P\downarrow (N_k^*\uparrow) | O_1^{\text{PV}} | \Sigma_k^*\downarrow(\Sigma\uparrow)\rangle = -\tfrac{1}{4}[(M_{VA}+M_{AV}) - (N_{VA}+N_{AV})]_{\Sigma_k^*(N_k^*)} , \tag{6a}$$

$$\langle P\downarrow (N_k^*\uparrow) | O_{2,3,4}^{\text{PV}} | \Sigma_k^*\downarrow(\Sigma\uparrow)\rangle = -\tfrac{1}{4}[(M_{VA}+M_{AV}) + (N_{VA}+N_{AV})]_{\Sigma_k^*(N_k^*)} , \tag{6b}$$

$$\langle P\downarrow (N_k^*\uparrow) | O_5^{\text{PV}} | \Sigma_k^*\downarrow(\Sigma\uparrow)\rangle = -\tfrac{2}{3}[M_{VA} - M_{AV}]_{\Sigma_k^*(N_k^*)} , \tag{6c}$$

TABLE I. Operators entering Eq. (3).

C_iO_i	Operators SU(3) flavor and isospin content	$(\bar{d}s)\ (\bar{u}u)$	$(\bar{d}u)\ (\bar{u}s)$	$(\bar{d}s)\ (\bar{d}d)$	$(\bar{d}s)\ (\bar{s}s)$
		Four-quark combinations $(\bar{q}_L^{1i}\gamma_\mu q_L^{2i})\ (\bar{q}_L^{3j}\gamma_\mu q_L^{4j})$			
C_1O_1	$\underline{8}_f$, $\Delta I=\frac{1}{2}$	C_1	$-C_1$	0	0
C_2O_2	$\underline{8}_d$, $\Delta I=\frac{1}{2}$	C_2	C_2	$2C_2$	$2C_2$
C_3O_3	$\underline{27}$, $\Delta I=\frac{1}{2}$	C_3	C_3	$2C_3$	$-3C_3$
C_4O_4	$\underline{27}$, $\Delta I=\frac{3}{2}$	C_4	C_4	$-C_4$	0
		$(\bar{q}_L^{1i}\gamma_\mu\lambda_a^{ij}q_L^{2j})\ (\bar{q}_R^{3k}\lambda_a^{kl}\gamma_\mu q_R^{4l})$			
C_5O_5	$\underline{8}$, $\Delta I=\frac{1}{2}$	$C_5[(\bar{d}_L\lambda_a s_L)(\bar{u}_R\lambda_a u_R+\bar{d}_R\lambda_a d_R+\bar{s}_R\lambda_a s_R)]$			
C_6O_6	$\underline{8}$, $\Delta I=\frac{1}{2}$	$C_6[(\bar{d}_L s_L)(\bar{u}_R u_R+\bar{d}_R d_R+\bar{s}_R s_R)]$			

$$\langle P\!\downarrow\!(N_k^*\!\uparrow)|O_6^{\rm PV}|\Sigma_k^*\!\downarrow\!(\Sigma\!\uparrow)\rangle=\tfrac{1}{4}[M_{VA}-M_{AV}]_{\Sigma_k^*(N_k^*)}\,. \quad (6d)$$

In Table II we list the resulting matrix elements $E(\Sigma_k^*)$ $[E(N_k^*)]$ of expression (3) for the set of resonances considered.

IV. ELECTROMAGNETIC VERTICES

The electromagnetic transition $N^*\to p\gamma$ $(\Sigma^+\to\Sigma^*\gamma)$ is a counterpart of the weak transition (5) and, on a general symmetry ground, is of the form

$$H_{\rm EM}(x)=\sum_{N^*}\left(\frac{\mu_T(N^*)}{2}\bar{\Psi}_{N^*}(x)\sigma_{\mu\nu}\gamma_5\Psi_p(x)F_{\mu\nu}(x)+\text{H.c.}\right)+\sum_{\Sigma^*}\left(\frac{\mu_T(\Sigma^*)}{2}\bar{\Psi}_{\Sigma^*}(x)\sigma_{\mu\nu}\gamma_5\Psi_\Sigma(x)F_{\mu\nu}(x)+\text{H.c.}\right). \quad (7)$$

Therefore, let us call μ_T the magnetic moment of the $(\frac{1}{2}^{\mp}\to\frac{1}{2}^{\pm})$ (i.e., $p_{1/2}\leftrightarrow s_{1/2}$) transition. We use the usual procedure[14,15] for calculating the matrix elements of two-quark operators appearing in the quark electromagnetic current. First, we calculate the emission of a photon at the quark level. Single-quark matrix elements describing the absorption of a helicity +1 photon can be easily expressed by the helicity amplitudes $A_{1/2}^i$ (Refs. 7,15),

$$A_{1/2}^i=\frac{1}{\sqrt{2k}}\langle\tfrac{1}{2}^-\!\uparrow|\vec{\epsilon}^{\,(+)}\cdot\vec{J}_i^{\rm EM}|\tfrac{1}{2}^+\!\downarrow\rangle\,. \quad (8)$$

Here i denotes light (l) and strange (s) quarks, and the electromagnetic current operator in the bag has the usual form

$$\vec{\epsilon}^{\,(+)}\cdot\vec{J}_i^{\rm EM}=\int_{\rm bag}d^3r\,q_i^\dagger(r)\vec{\epsilon}^{\,(+)}\cdot\vec{\alpha}Q_iq_i(r)e^{i\vec{k}\cdot\vec{r}}\,. \quad (9)$$

For completeness, let us write the magnetic moment of the $(\frac{1}{2}^+\to\frac{1}{2}^+)$ (i.e., $s_{1/2}\to s_{1/2}$) single-quark transition[14] expressed over radial integrals listed in (A4):

$$\mu_i(\tfrac{1}{2}^+\to\tfrac{1}{2}^+)=e\frac{N^2}{2k}(R_{01}^1+R_{10}^1)\,. \quad (10)$$

TABLE II. Resonances with the quark content (tilde denotes the quark in the p state), masses in GeV, and radii in GeV^{-1}. The effective weak vertices are calculated for two sets of bag-model parameters and for two choices of integration radius, as explained in the Appendix.

$\frac{1}{2}^-$ resonance[a]	Quarks	M	R	E (10^{-7} GeV) (i) Bag model[a,b] Solution A	Solution B	(ii) Bag model[c] Solution A	Solution B
N_a	$(u\tilde{u}d, uu\tilde{d})$	1.327	5.613	1.0462	0.8792	0.3545	0.3206
N_b	$(u\tilde{u}d, uu\tilde{d})$	1.275	5.539	0.4878	0.4030	0.1679	0.1412
Δ	$(u\tilde{u}d, uu\tilde{d})$	1.362	5.663	0.0932	0.0372	0.0107	0.0086
Σ_1	$(uu\tilde{s})$	1.445	5.569	0.3180	0.2590	0.1022	0.0830
Σ_a	$(u\tilde{u}s)$	1.517	5.607	0.4480	0.3687	0.1506	0.1237
Σ_b	$(u\tilde{u}s)$	1.473	5.513	−0.6149	−0.5081	−0.2076	−0.1707

[a] Reference 13.
[b] Reference 6.
[c] Reference 7.

An analogous expression for the magnetic moment of the transition we are considering is of the form [see (A5)–(A7)]

$$\mu_i(\tfrac{1}{2}^{\mp}\to\tfrac{1}{2}^{\pm})=e\frac{N\tilde{N}}{2k}(\tilde{R}^0_{00}-\tfrac{1}{3}\tilde{R}^0_{11}+\tfrac{2}{3}\tilde{R}^2_{11})\,. \tag{11}$$

Here the $\frac{1}{2}^- - \frac{1}{2}^+$ (i.e., $p_{1/2}$-$s_{1/2}$) relative phase is already incorporated.

Second, we consider hadronic transitions. The magnetic moment for hadronic transitions receives contributions from the magnetic moments of light and strange quarks,

$$\mu_T=\chi_l\mu_l+\chi_s\mu_s\,. \tag{12}$$

To conclude, in Table III we list the values of transition magnetic moments and the values of hadronic factors χ_i for all resonances of interest.

V. RESULTS AND DISCUSSION

Expressions (1) enable us to calculate the expected value of the PV amplitude using the empirical values of asymmetry and decay rate.[12] The experimental value of the PV amplitude is

$$|D|=1.24\times10^{-7}\ \mathrm{GeV}^{-1}\,.$$

This value is about 2.5 times larger than the value (0.5×10^{-7} GeV^{-1}) calculated in Ref. 2. According to Eq. (2), our predictions for this quantity follow from the results of the preceding sections. Following the two chains of calculations of polarized-Σ^+ decay in Tables II and III, namely,

$$\text{(a)}\quad \Sigma^+\uparrow \xrightarrow[\mathrm{W}]{} N^*\uparrow \xrightarrow[\mathrm{EM}]{} p\downarrow+\gamma$$

and

$$\text{(b)}\quad \Sigma^+\uparrow \xrightarrow[\mathrm{EM}]{} \gamma+\Sigma^*\downarrow \xrightarrow[\mathrm{W}]{} p\downarrow+\gamma\,,$$

we summarize final results in Table IV. These are rather close to the experimental value.

Note that the values of amplitudes in Table IV are entirely predicted by choice (i) given in the Appendix, because the masses of resonances we are considering are also calculated for this choice. It is evident from Tables II and III that choice (ii) leads to somewhat lower values.

We should also note that the main role in the total contribution in Table IV is played by the resonance N_b as given in Ref. 13. Obviously, the mixing of states [see (A2)] is of importance. To gain an insight into the meaning of our calculation, we compare some other empirically known quantities (Table V). Apparent disagreement as seen in the last row of Table V might be due to the problem with the matching between theoretical and experimental $\frac{1}{2}^-$ resonances. It is well known that the MIT bag model predicts more $\frac{1}{2}^-$ states than found empirically (see Sec. II). Thus it would be quite possible to match $N_b(S''_{11})$ what would lead to too small results. In view of these problems it seemed most consistent to employ theoretical magnetic moments (12) in combination with the theoretical $\frac{1}{2}^-$ states.

The results listed in the Table IV are encouraging. They indicate that the QCD-renormalized Weinberg-Salam model combined with the MIT bag model, implemented by $\frac{1}{2}^-$ resonances, may also be important in explaining the weak electromagnetic PV amplitude considered. Irrespective of relatively large experimental uncertainties ($\alpha=-1.03^{+0.52}_{-0.42}$), there is no doubt that $\frac{1}{2}^-$ resonance poles should be taken into account. Moreover, the inclusion of $\frac{1}{2}^-$ resonances can explain the PV (D) amplitude measured for the radiative weak decay $\Sigma^+\to p\gamma$.

TABLE III. Transition magnetic moments for the resonances and the choices of bag-model parameters as in Table II. The hadronic factors χ resulting from the overlap of quark operators between baryon states are also listed.

			μ_T (e GeV^{-1})			
			(i) Bag model[a,b]		(ii) Bag model[c]	
			Solution A	Solution B	Solution A	Solution B
		$\mu_l=$	0.5532	0.5569	0.5743	0.5801
$\frac{1}{2}^-$ resonance[a]	$(\chi_l;\chi_s)$	$\mu_s=$	0.5015	0.5	0.4833	0.4801
N_a	(0.0236;0)		0.0130	0.0131	0.0135	0.0137
N_b	(−0.6647;0)		−0.3677	−0.3702	−0.3817	−0.3856
Δ	(−0.0428;0)		−0.0237	−0.0238	−0.0246	−0.0248
Σ_1	(0;−0.0370)		−0.0186	−0.0185	−0.0179	−0.0178
Σ_a	(−0.2113;0)		−0.1168	−0.1176	−0.1213	−0.1225
Σ_b	(−0.4656;0)		−0.2576	−0.2593	−0.2674	−0.2701

[a] Reference 13.
[b] Reference 6.
[c] Reference 7.

TABLE IV. PV amplitudes calculated according to Eqs. (2a) and (2b) for nonstrange and strange $\frac{1}{2}^-$ baryons, respectively.

$\frac{1}{2}^-$ resonance[a]	$m_{N^*(\Sigma)} - m_{\Sigma^+(p)}$(GeV)	D (10^{-7} GeV^{-1}) for (i) bag model[a,b] Solution A	Solution B
N_a	0.183	−0.074	−0.063
N_b	0.131	1.369	1.139
Δ	0.218	0.010	0.004
Σ_1	0.507	0.015	0.012
Σ_a	0.579	0.090	0.075
Σ_b	0.535	0.296	0.246
Total contribution		1.496	1.239

[a] Reference 13.
[b] Reference 6.

ACKNOWLEDGMENTS

It is a pleasure to thank Professor D. Tadić for introducing me to the subject and for stimulating discussions. This work was supported by SIZ I, Zagreb, Croatia, Yugoslavia.

APPENDIX

The renormalization coefficients appearing in Eq. (3) are the same as in Ref. 5:

$$\begin{aligned} &C_1 = -2.410, \quad C_2 = 0.089, \quad C_3 = 0.085, \\ &C_4 = 0.423, \quad C_5 = -0.063, \quad C_6 = -0.014. \end{aligned} \tag{A1}$$

The $\frac{1}{2}^-$ resonance states N_1, N_2, Δ, Σ_1, Σ_2, and Σ_3 are taken from Ref. 13. We list only the state-mixing matrices which determine the "hadronic factors" in Table III; they are as follows:

$$\begin{pmatrix} N_a \\ N_b \end{pmatrix} = \begin{pmatrix} 0.68 & 0.73 \\ 0.73 & -0.68 \end{pmatrix} \begin{pmatrix} N_1 \\ N_2 \end{pmatrix}, \tag{A2}$$

$$\begin{pmatrix} \Sigma_a \\ \Sigma_b \end{pmatrix} = \begin{pmatrix} 0.81 & 0.58 \\ 0.58 & -0.81 \end{pmatrix} \begin{pmatrix} \Sigma_2 \\ \Sigma_3 \end{pmatrix}. \tag{A3}$$

We have used two versions of the bag model:

(i) the one corresponding to Ref. 6 and also used in Ref. 13 and

(ii) the other referring to Ref. 7.

The outstanding problem in calculating nondiagonal matrix elements in the bag model is the choice of the radius of integration. The two logical possibilities used in the fixed-sphere bag model are $R = \min(R_1, R_2)$ and $R = \frac{1}{2}(R_1 + R_2)$. In Table VI we denote them as Solution A and Solution B. For each choice of the "characteristic radius" in Table VI we recalculate the eigenfrequencies and replace R_1 and R_2 by R. Such an ansatz for calculating the transition bag matrix elements was motivated and used in Ref. 14. In this way, we can calculate the radial integrals which determine the electromagnetic transition moments (10) and (11). For example, the transition moment and the decay rate of $\Sigma^0 \to \Lambda\gamma$[14] are entirely determined by

$$R_{01}^1 = R_{10}^1 = \int_0^R dr\, r^2 j_1(kr) j_1(pr) j_0(pr). \tag{A4}$$

The absolute values of the predicted and measured moments are compared in Table V.

TABLE V. Model predictions of some measured quantities.

Hadronic quantity		Predicted value (i) A	(i) B	(ii) A	(ii) B	Measured value	Reference
Transition moment $\lvert\mu_{\Sigma^0\Lambda}\rvert$ (e GeV^{-1})		0.573	0.611	0.785	0.834	$0.97^{+0.13}_{-0.10}$	16
Helicity amplitudes $\lvert A_{1/2}\rvert$ (GeV$^{-1/2}$)	$N_a(S_{11}'')$	0.012	0.012	0.013	0.013	0.044 ± 0.024	12
	$N_b(S_{11}')$	0.349	0.351	0.362	0.365	0.064 ± 0.019	

TABLE VI. Values of bag-model parameters and the choices used in preparing Tables II and III.

Bag model	Solution	R (GeV^{-1})	ω_l	ω_s	$\tilde{\omega}_l$	$\tilde{\omega}_s$
(i) References 6 and 13 (GeV)	A	4.950	2.0428	2.8430	3.8115	4.1806
$B^{1/4}=0.147$ $m_l=0$, $m_s=0.279$	B	5.285	2.0428	2.9059	3.8115	4.2201
(ii) Reference 7 (GeV)	A	7.25	2.2033	3.3946	3.8576	4.5541
$B^{1/4}=0.1139$ $m_l=0.0441$, $m_s=0.2978$	B	7.75	2.2151	3.5066	3.8617	4.6363

In Table V we also compare the calculated and measured[12] absolute values of helicity amplitudes. The relevant integrals are

$$\tilde{R}^0_{00}=\int_0^R dr\, r^2 j_0(kr) j_0(pr) j_0(\tilde{p}r)\,, \tag{A5}$$

$$\tilde{R}^0_{11}=\left[\frac{(\omega-mR)(\tilde{\omega}+mR)}{(\omega+mR)(\tilde{\omega}-mR)}\right]^{1/2} \times\int_0^R dr\, r^2 j_0(kr) j_1(pr) j_1(\tilde{p}r)\,, \tag{A6}$$

$$\tilde{R}^2_{11}=\left[\frac{(\omega-mR)(\tilde{\omega}+mR)}{(\omega+mR)(\tilde{\omega}-mR)}\right]^{1/2} \times\int_0^R dr\, r^2 j_2(kr) j_1(pr) j_1(\tilde{p}r)\,. \tag{A7}$$

Here k is the photon momentum, $p=(1/R)(\omega^2-m^2R^2)^{1/2}$, and the tilde marks p-state quantities.

In addition, neutron-electric-dipole-moment calculations[17] show indirectly that the description of $\frac{1}{2}^-$ resonance states in the framework of the MIT bag model leads to reasonable estimates of their matrix elements.

[1] F. J. Gilman and M. B. Wise, Phys. Rev. D 19, 976 (1979).

[2] Riazuddin and Fayyazuddin, Report No. IC/79/54, ICTP, Trieste, 1979 (unpublished).

[3] L. K. Gershwin *et al.*, Phys. Rev. 188, 2077 (1969).

[4] M. A. Ahmed and G. G. Ross, Phys. Lett. 59B, 293 (1975); N. Vasanti, Phys. Rev. D 13, 1889 (1976); M. A. Shifman, A. I. Vainshtein, and V. I. Zakharov, Report No. ITEP-113, 1976 (unpublished); Phys. Rev. D 18, 2583 (1978).

[5] A. I. Vainshtein, V. I. Zakharov, and M. A. Shifman, Zh. Eksp. Teor. Fiz. 72, 1275 (1977) [Sov. Phys.—JETP 45, 670 (1977)]; Reports Nos. ITEP-63 and ITEP-64, 1976 (unpublished); M. A. Shifman, A. I. Vainshtein, and V. I. Zakharov, Nucl. Phys. B120, 316 (1977).

[6] A. Chodos, R. L. Jaffe, K. Johnson, C. B. Thorn, and V. F. Weisskopf, Phys. Rev. D 9, 3471 (1974); A. Chodos, R. L. Jaffe, K. Johnson, and C. B. Thorn, *ibid.* 10, 2599 (1974); T. A. De Grand, R. L. Jaffe, K. Johnson, and J. Kiskis, *ibid.* 12, 2060 (1975).

[7] J. F. Donoghue, E. Golowich, and B. R. Holstein, Phys. Rev. D 12, 2875 (1975).

[8] H. Galić, D. Tadić, and J. Trampetić, Nucl. Phys. B158, 306 (1979); J. F. Donoghue, E. Golowich, W. R. Ponce, and B. R. Holstein, Phys. Rev. D 21, 186 (1980); H. Galić, D. Tadić, and J. Trampetić, Phys. Lett. 89B, 249 (1980).

[9] R. E. Marshak, Riazuddin, and C. P. Ryan, *Theory of Weak Interactions in Particle Physics* (Wiley-Interscience, New York, 1969).

[10] D. Palle, I. Picek, D. Tadić, and J. Trampetić, Nucl. Phys. B166, 149 (1980).

[11] R. H. Graham and S. Pakvasa, Phys. Rev. 140, B 1144 (1965); G. Farrar, Phys. Rev. D 4, 212 (1971); B. Holstein, Nuovo Cimento 2A, 561 (1971); M. D. Scadron and L. R. Thebaud, Phys. Rev. D 8, 2190 (1973).

[12] Particle Data Group, Phys. Lett. 75B, 1 (1978).

[13] T. A. De Grand and R. L. Jaffe, Ann. Phys. (N.Y.) 100, 425 (1976).

[14] R. H. Hackman, N. G. Deshpande, D. A. Dicus, and V. L. Teplitz, Phys. Rev. D 18, 2537 (1979).

[15] A. J. G. Hey, B. R. Holstein, and D. P. Sidhu, Ann. Phys. (N.Y.) 117, 5 (1979).

[16] F. Dydak *et al.*, Nucl. Phys. B118, 1 (1977); F. J. Gilman, in *Quark Spectroscopy and Hadron Dynamics*, proceedings of the SLAC Summer Institute on Particle Physics, 1977, edited by M. C. Zipf (SLAC, Stanford, 1977), p. 121; R. B. Teese and R. Settles, Phys. Lett. 87B, 111 (1979).

[17] V. Baluni, Phys. Rev. D 19, 2227 (1979); R. J. Crewther, P. Di Vecchia, G. Veneziano, and E. Witten, Phys. Lett. 88B, 123 (1979).